# Assignment and Charge Translocation Stoichiometries of the Major Electrogenic Phases in the Reaction of Cytochrome *c* Oxidase with Dioxygen†

Audrius Jasaitis,‡ Michael I. Verkhovsky, Joel E. Morgan, Marina L. Verkhovskaya, and Mårten Wikström*

*Department of Medical Chemistry, Institute of Biomedical Sciences, P.O. Box 8 (Siltavuorenpenger 10), University of Helsinki, FIN-00014 Helsinki, Finland*

*Received September 22, 1998; Revised Manuscript Received December 17, 1998*

ABSTRACT: The reaction of cytochrome *c* oxidase with dioxygen has been studied by means of time-resolved measurements of electrical membrane potential ($\Delta\Psi$). Microsecond time resolution was achieved by starting with the CO-inhibited enzyme, which was photolyzed after addition of oxygen. The time course of the reaction could be fitted by using a five-step sequential reaction as a model. The first two phases of the reaction, which correspond in time to binding of oxygen followed by formation of the P (peroxy) intermediate, as observed spectroscopically, are not associated with net charge displacement across the membrane. After this lag, $\Delta\Psi$ develops in three phases, which correspond in time to the conversion of P to the F (ferryl) intermediate, in a single phase, and conversion of F to O (the fully oxidized enzyme), in two phases. The amplitude of $\Delta\Psi$ was approximately equal for the P → F and F → O portions of the reaction. When the oxygen reaction is started with incompletely reduced enzyme, it will halt at the P or F state. When the reaction was allowed to proceed to the F state, but no further, only the fast phase of $\Delta\Psi$ formation was observed, whereas no $\Delta\Psi$ was generated if the reaction was halted at P. This finding places the assignments of phases in the electrometric data on a firmer basis—they are no longer based solely on temporal correspondence with phases in the spectroscopic data. To define the number of charges transferred across the membrane during the reaction, some kind of calibration is needed. For this purpose, another type of reaction—electron transfer following CO photolysis in the absence of oxygen ("backflow")—was studied. Parallel spectroscopic and electrometric measurements showed that the fast electron transfer from the low-spin heme to $Cu_A$ in the backflow process results in approximately 11 times smaller amplitude of $\Delta\Psi$ as compared with $\Delta\Psi$ generated in the reaction of the reduced enzyme with oxygen (the polarity is also reversed). If it is assumed that transfer of an electron from the low-spin heme to $Cu_A$ amounts to movement of a unit charge across half of the membrane dielectric, charge translocation in the reaction of the reduced enzyme with oxygen amounts to approximately 5.5 unit charges—the value predicted if all four protons pumped during the catalytic cycle are translocated during the oxidative part of the reaction.

Cytochrome *c* oxidase is a biological energy transducer. The enzyme catalyzes the reduction of molecular oxygen to produce water, consuming four electrons and four protons in the process. However, the most important product is the free energy released in the reaction, which is used to create and maintain an electrochemical proton gradient ($\Delta\mu_{H^+}$)[1] across the inner mitochondrial membrane. This membrane gradient drives the formation of ATP, which ultimately supplies most of the energy needs of the cell.

There are two aspects to the process by which cytochrome *c* oxidase generates this electrochemical proton gradient. Half of the energy conservation is a direct consequence of the way that the chemistry of oxygen reduction is arranged in the membrane. The four electrons required for the reaction are donated by cytochrome *c*, and enter the enzyme from the outer side of the membrane, while the four protons are taken from the inner side. In this way, reduction of one molecule of oxygen to two water molecules has an effect equivalent to moving four electrical charges all the way across the membrane dielectric. In addition, the enzyme is an electrogenic proton pump; for every molecule of oxygen reduced to water, an additional four protons are translocated from the inner side of the membrane to the outer side (*2*).

The general structure of the enzyme—helix topology and the assignment of metal ligands—was determined by biochemical and site-directed mutagenesis studies (*3*, *4*). This

† Supported by grants from The Academy of Finland, The University of Helsinki, Biocentrum Helsinki, and the Center for International Mobility.

‡ On leave from the Vytautas Magnus University, Daukanto 28, 3000 Kaunas, and Institute of Biochemistry, Moksliniku 12, 2600, Vilnius, Lithuania.

[1] Abbreviations: A, ferrous-oxy compound of $Fe_{a3}$; BTP, Bis-tris propane; $\delta$, interaction between redox centers; DCPIP, dichlorophenol-indophenol; $d_{HM}$, the "Hinkle−Mitchell" parameter, effective depth of $Fe_a$ in membrane dielectric (see Discussion); $\Delta\mu_{H^+}$, electrochemical membrane proton gradient; $\Delta\Psi$, electrical membrane potential; $E_h$, redox potential; $E_m$, midpoint redox potential; NHE, normal hydrogen electrode; F, ferryl intermediate; $Fe_a$, low-spin heme; $Fe_{a3}$, oxygen-binding heme; *k*, rate constant; O, fully oxidized form of binuclear oxygen reduction site; P, "peroxy" intermediate; R, unliganded, fully reduced enzyme; RT, room temperature; $Ru(bipy)_3$, tris(2,2′-bipyridyl)-ruthenium; $\tau$, time constant ($t_{1/e}$); TMPD, *N*,*N*,*N*′,*N*′-tetramethyl-1,4-phenylenediamine.

10.1021/bi982275l CCC: $18.00 © 1999 American Chemical Society
Published on Web 02/09/1999

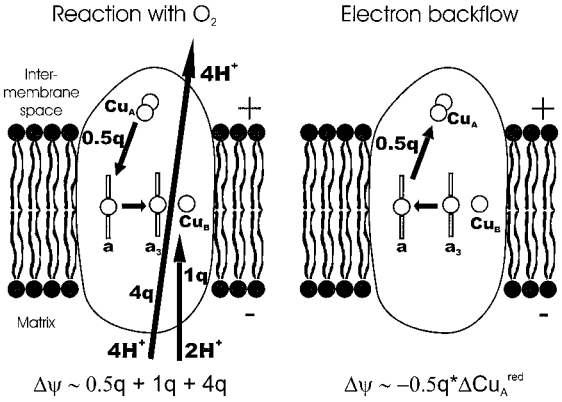


FIGURE 1: Schematic representation of cytochrome *c* oxidase illustrating the relative positions of redox centers in the membrane and showing charge movement under two different types of experimental conditions: left panel, reaction of fully reduced enzyme with oxygen; right panel, redistribution of electrons after photolysis of CO in the CO mixed-valence enzyme. The scheme incorporates the assumptions that the hemes are located halfway through the dielectric ($d_{HM} = 0.5$; see Discussion) and that four protons are pumped during the oxidative part of the enzyme cycle. On the basis of these assumptions, the reaction of fully reduced enzyme with oxygen would translocate 5.5 charges across the membrane: four protons pumped across the entire dielectric (4.0), two protons taken up through half of the membrane ($2 \times 0.5 = 1.0$), and one electron from $Cu_A$ moving across half of the dielectric (0.5). In the backflow reaction, as drawn, electrons would have to cross half the dielectric to reach $Cu_A$. $\Delta Cu_A$ represents the fraction of $Cu_A$ that becomes reduced—12% maximally.

was later confirmed and extended to atomic detail when the enzyme was crystallized (*5*, *6*). However, a great deal of our knowledge of the enzyme, including the flow path for electrons, comes from kinetic studies. The point of entry for electrons is $Cu_A$, a binuclear copper center[2] and a one-electron carrier, which is situated near the membrane surface (*7*, *8*). As shown in Figure 1, electrons flow from $Cu_A$ to $Fe_a$, a low-spin heme, and then to a binuclear iron−copper site ($Fe_{a3}Cu_B$) where the chemistry of oxygen reduction takes place. $Fe_a$, $Fe_{a3}$, and $Cu_B$ are all buried in the membrane.

The fully reduced enzyme contains four reducing equivalents—the number required for the reduction of one oxygen molecule to two waters. This reaction reaches completion in a few milliseconds, but within this time at least four different kinetic phases can be resolved. Typically, to obtain the necessary time resolution, the reaction is initiated by first mixing the CO-inhibited enzyme with oxygen in the dark and then photolyzing the CO with a flash of light (*9*).

In broad outline, the reaction takes place as follows: Immediately after CO photolysis the reduced enzyme (R) binds oxygen rapidly ($\tau = 8\ \mu$s, $k = 1.25 \times 10^5\ s^{-1}$, $[O_2] = 1$ mM, RT; *10*, *11*) to form a ferrous-oxy intermediate (A). Redox chemistry begins in the next step ($\tau = 32\ \mu$s, $k = 3.1 \times 10^4\ s^{-1}$, $[O_2] = 1$ mM, RT; *11*) with oxidation of the $Fe_a$ (*8*, *12*−*14*) and formation of what is believed to be a formal "peroxy" intermediate (P, or $P_R$ to distinguish this from a similar oxygen intermediate formed by the reaction of oxygen with the half-reduced enzyme; see ref *15*). At this point three of the four redox equivalents that will be needed for the reduction of oxygen to water are resident in the binuclear site, while the fourth electron is still on $Cu_A$; $Fe_a$ is oxidized. In the next phase ($\tau = 140\ \mu$s, $k = 7 \times 10^3\ s^{-1}$; RT, *12*), $P_R$ becomes reduced to an oxy-ferryl species (F; *16*−*18*). At the same time $Cu_A$ becomes partially oxidized as the fourth electron equilibrates between $Cu_A$ and $Fe_a$ (*8*). Finally, in a much slower process ($\tau \sim 1$ ms), the remaining electron, shared between $Cu_A$ and $Fe_a$, migrates to the binuclear center, resulting in the conversion of F into the fully oxidized enzyme (O) (*8*).

Thus, the reaction proceeds from the reduced enzyme (R) through "peroxy" (P) and ferryl (F) intermediates to the fully oxidized enzyme (O). The P and F intermediates have also been identified in experiments in which this reaction was reversed. Wikström showed that by placing a backward driving force on the enzyme in mitochondria ($\Delta\Psi$ and high $E_h$), the oxygen reaction could be partially reversed from the O state, leading first to F and then to P (*19*, *20*). Thermodynamic analysis of this reaction led to the conclusion that all the work required for proton pumping is done in the two electron-transfer steps: P → F and F → O, consistent with translocation of two protons at each step (*21*).

In the present study we have repeated and extended our earlier electrometric measurements on the reaction of reduced cytochrome *c* oxidase with oxygen (*22*). We confirm that $\Delta\Psi$ develops in two roughly equal parts, in phases that correspond in time to the P to F and F to O transitions, observed spectroscopically—the transitions between R and P are essentially electrically silent. We show that when the reaction is prematurely curtailed at P or F, the growth of $\Delta\Psi$ is correspondingly curtailed, confirming that the association between transitions in the oxygen chemistry and phases in the growth of $\Delta\Psi$ is not an accident of timing. Finally, as a calibration, we establish the relationship between the amount of net charge translocation in this reaction and the amount of charge that moves during a well-defined internal electron-transfer reaction of the enzyme.

## MATERIALS AND METHODS

*Reagents.* Lipids for preparation of liposomes and for the electrometric measuring membranes were either L-lecithin 20% [plant] (Avanti Polar Lipids, Alabaster, AL) or L-lecithin type IV-S [soybean] (Sigma). Catalase (from bovine liver), cytochrome *c* (from horse heart), and glucose oxidase (type VII, from *Aspergillus Niger*) were from Sigma.

*Enzyme Preparation.* Bovine heart cytochrome *c* oxidase was prepared by a modification of the method of Hartzell and Beinert (*23*). During enzyme preparation, the pH was kept above 7.8 and Triton X-114 and cholate were added on the basis of cytochrome $aa_3$ concentration rather than total protein (*24*). No ethanol was used to remove the Triton X-114 after the red/green cut; instead, the green pellet was repeatedly resuspended in the preparation buffer and centrifuged, until the amount of detergent was significantly reduced, as judged by the extent of bubbling when the supernatant was shaken (usually three or four exchanges).

*Reconstitution of the Enzyme into Phospholipid Vesicles.* To remove cytochrome *c* oxidase dimers and other possible

[2] Nomenclature: In cytochrome *c* oxidase (cytochrome $aa_3$; EC 1.9.3.1) the low-spin heme is known as heme *a* or $Fe_a$ and the oxygen-binding heme is known as heme $a_3$ or $Fe_{a3}$ (in both, the chemical entity is heme A). The copper ion of the oxygen-reduction site is known as $Cu_B$. An additional bimetallic copper site known as $Cu_A$ serves as the initial electron acceptor from cytochrome *c*. The related quinol oxidases do not contain $Cu_A$ (*1*).

Table 1: Protocol for Detergent Removal

| time, min | amount of Bio-Beads added (mg/mL) | temperature |
|---|---|---|
| 0 | 33.2 | 4 °C |
| 30 | 33.2 | 4 °C |
| 60 | 33.2 | 4 °C |
| 90 | 33.2 | 4 °C |
| 120 | 66.5 | 4 °C |
| 180 | 66.5 | 4 °C |
| 240 | 133 | RT[b] |
| 270 | 133 | RT |
| 300 | 266[a] | RT |
| 360 | 266 | RT |
| 420 | ready | RT |

[a] In this case, 0.5 mL of 100 mM potassium-HEPES, pH 7.4, was also added. [b] RT, room temperature.

contaminants from the preparation, the enzyme was purified on a sucrose gradient as described by Finel and Wikström (*25*). Reconstitution of enzyme into proteoliposomes was carried out as follows: 150 $\mu$L of cytochrome *c* oxidase from the gradient (concentration approximately 4−8 $\mu$M) was diluted to a volume of 1 mL with a suspension of sonicated, preformed liposomes containing 80 mg/mL lipid, 2% (w/v) cholic acid, and 100 mM potassium-HEPES (pH 7.4) and was mixed for 20 min at room temperature. Removal of detergent was performed according to Rigaud et al. (*26*) using Bio-Beads SM-2 absorbent (Bio-Rad). The scheme for detergent removal is shown in Table 1. It should be noted that, to slow the removal of detergent, the first few additions of Bio-Beads were performed at 4 °C. This increased the yield of reconstituted enzyme. At the end of the procedure, vesicles with a respiratory control ratio of 15−20 were typically obtained. Proteoliposomes were frozen and stored in liquid nitrogen. The final concentration of enzyme in the vesicles, determined spectrophotometrically using $\epsilon_{604-620}$-(reduced−oxidized) = 0.024 cm$^{-1}$ $\mu$M$^{-1}$, was typically 0.3−0.5 $\mu$M.

*Measurement Procedure.* The direct, time-resolved electrical measurement is based on a method originally developed by Drachev et al. (*27*, *28*). In the present system Ag/AgCl$_2$ electrodes record the voltage between the two compartments of a cell, separated by a measuring membrane, consisting of a lipid-impregnated Teflon mesh. Vesicles, into which the enzyme has been reconstituted, are forced to associate with this measuring membrane (see Figure 2 in ref *22*). The voltage across the measuring membrane follows the $\Delta\Psi$ across the vesicle membranes proportionally, allowing the kinetics of charge translocation to be recorded. Typically the measuring membrane has a resistance of about 5 G$\Omega$ and the measured $\Delta\Psi$ decays with a time constant of about 5 s.

*Preparation of Samples.* Proteoliposomes were added to the one of two compartments of the cell and were forced to associate with the measuring membrane by addition of 10−15 mM CaCl$_2$ (the same amount of CaCl$_2$ was added to both compartments) followed by an incubation of between 2 and 3 h. Incubation was carried out at pH 7 (usually in 100 mM BTP). The cell was enclosed in a gas tight box which had been purged with argon and anaerobicity was reached by addition of 50 mM glucose, 50 $\mu$g/mL catalase, and 130 $\mu$g/mL glucose oxidase. After incubation, the cell was removed from the box and the liquid in both compartments was exchanged for argon-bubbled buffer (usually 100 mM HEPES, pH 8). Immediately thereafter, 50 mM glucose, 50 $\mu$g/mL catalase, and 130 $\mu$g/mL glucose oxidase were added to keep the sample anaerobic. Then 100 $\mu$M TMPD, 100 $\mu$M DCPIP, 10 $\mu$M hexaammineruthenium, and 0.5 $\mu$M cytochrome *c* were added as redox mediators, and 60 mM of ferrocyanide was used as a redox buffer. After all additions, Ag/AgCl$_2$ electrodes (World Precision Instruments, Stevenage, Hertfordshire, U.K.) that had been kept in an anaerobic environment were inserted, and the cell was returned to the gas tight box, which was then purged with argon followed by CO (100%). A computer-driven syringe pump (SP200i, World Precision Instruments) was used to inject 50 $\mu$L of oxygen-saturated buffer (rate 5 mL/min) via a 2.5 mL gas tight syringe and a long 22S RN needle (Hamilton, Reno, NV). The jet from the needle was directed at the measuring membrane (a 4 mm circle), producing a local high concentration of oxygen for the time of the reaction. The reaction was started by a laser flash (Quantel Brilliant frequency-doubled YAG, pulse energy 180 mJ) 200 ms after the end of the injection. The oxygen concentration at the membrane after injection is almost certainly close to the saturation value of 1.2 mM, because increasing the injected volume does not decrease the lag or increase the rate of the "fast" phase (see below) and the rates obtained by fitting are consistent with those from optical data obtained at close to saturating oxygen concentrations. For experiments in which the redox potential ($E_h$) of the medium was titrated, the $E_h$ was initially raised by the addition of a small volume of concentrated anaerobic ferricyanide. After that, the glucose−glucose oxidase system itself slowly lowered the $E_h$, and kinetic measurements could be initiated when the appropriate $E_h$ values were reached. The $E_h$ of the system was determined from the voltage between a platinum wire (measuring electrode) and the ground Ag/AgCl$_2$ electrode (reference electrode, +200 mV vs NHE).

*Measurement Electronics.* The measurement system consisted of a homemade operational preamplifier whose output could be recorded by using two different types of IBM PC-based digitizers: an 8-bit PCIP−SCOPE (Metrabyte) running DA90 acquisition software (Alexander Drachev, Tempe, AZ) and a 12-bit CompuScope 512 (Gage Applied Sciences, Montreal, Canada) running GageScope data acquisition software. Timing was controlled by a CTM-05 counter-timer board (Metrabyte).

*Sequential Reaction Model.* To fit the electrometric oxygen reaction data, a model of a sequential first-order chemical reaction with five steps was used. Each step in such a reaction is characterized by a first-order rate constant $k_i$ ($i$ = 1, ..., 5). The overall reaction can be characterized mathematically by a set of six differential equations where the six solutions represent the concentration of the six intermediates at any time. However, unlike a spectroscopic measurement, which tracks the formation and decay of the various reaction intermediates, the electrometric measurement tracks transport of charge across the membrane. The solutions of the differential equations each reflect the lifetime—formation and decay—of a given intermediate (the first solution shows only decay of the starting material and the last shows only the formation of the final product). These solutions cannot be used directly as a basis set to fit electrometric data because here, the quantity measured is net movement of charge, which does not necessarily move back in the next step; that

Scheme 1

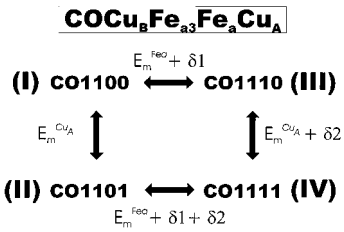


is, there is no process corresponding to obligatory decay of one intermediate as the next intermediate is formed. Thus, instead of using the solutions of the differential equations directly as the basis set for the fit, we constructed a cumulative sum of these solutions (1, 1 + 2, 1 + 2 + 3, ...) so that each vector in the basis set corresponds to the transition that takes place in one kinetic phase—in this case, the movement of one charge ($q$) through an arbitrary unit distance in the direction of the membrane normal. The rate constants and amplitudes were then varied to obtain the best fit to the experimental data with the *constr* constrained fitting function of MATLAB (Mathworks, South Natick, MA).

*Redox Titration of Backflow Measured Optically.* Optical measurements were carried out separately from the electrometric measurements by methods described earlier (*29*). Optical cuvettes with internal dimensions 10 mm × 10 mm (four windows polished), and constructed with joints for attachment to the vacuum line, were used. The two-electron reduced CO mixed-valence compound was made, in an optical cuvette, by incubating the oxidized enzyme under an anaerobic CO atmosphere (9 h, RT). The formation of pure mixed-valence (two-electron reduced) enzyme was judged by the optical absorption spectrum. The redox potential of the medium was titrated downward by illumination of the sample with a slide projector lamp. To follow the redox potential of the medium, 8 $\mu$M of cytochrome *c* was included in the sample. In calculations of redox potential of the medium a value of 260 mV (vs NHE) was used as the midpoint potential for cytochrome *c* (*30*).

The amount of $Cu_A$ that becomes reduced in the backflow experiments can be calculated from the data for 445 and 605 nm:

$$445\text{ nm:}\qquad x\epsilon_a^{445\text{nm}} + y\epsilon_{a_3}^{445\text{nm}} = A_{445\text{nm}} \tag{1}$$

$$605\text{ nm:}\qquad x\epsilon_a^{605\text{nm}} + y\epsilon_{a_3}^{605\text{nm}} = A_{605\text{nm}} \tag{2}$$

where the $A$ values are the measured absorbance changes for the slow phase of the reaction at 445 and 605 nm, $\epsilon_a$ and $\epsilon_{a_3}$ are extinction coefficients for $Fe_a$ and $Fe_{a_3}$ at 445 and 605 nm (*31*) and $x$ and $y$ are the molar concentrations of $Fe_a$ and $Fe_{a_3}$ that become oxidized. The sum $x + y$ gives the molar concentration of $Cu_A$ that becomes reduced.

*"Dark Titration" Model.* To describe the redox potential dependence of electron distribution among the redox centers of the enzyme with CO bound (before the laser flash), Scheme 1 was used. In this scheme there are four redox centers [$Cu_BFe_{a3}Fe_aCu_A$], each of which can be reduced (denoted 1) or oxidized (denoted 0). For example, in state I, CO is bound, maintaining the two metals of the binuclear center in the reduced state, while $Fe_a$ and $Cu_A$ remain oxidized. Hence, state I is denoted [CO1100]. Each transition in the scheme is associated with addition or removal of one electron. The redox potential of each transition is indicated next to the arrow; $E_m^{Fe_a}$, and $E_m^{Cu_A}$ denote the upper asymptotic potentials of $Fe_a$ and $Cu_A$, respectively. $\delta_1$ denotes the anticooperative redox interaction between the two hemes; $\delta_2$ denotes the anticooperative redox interactions between $Fe_a$ and $Cu_A$ (*32*−*35*). The redox behavior of this system can be described by the following set of equations:

$$\begin{cases} E_h = E_m^{Cu_A} + \dfrac{RT}{nF}\ln\dfrac{[I]}{[II]} \\ E_h = E_m^{Fe_a} + \delta_1 + \dfrac{RT}{nF}\ln\dfrac{[I]}{[III]} \\ E_h = E_m^{Cu_A} + \delta_2 + \dfrac{RT}{nF}\ln\dfrac{[III]}{[IV]} \\ [I] + [II] + [III] + [IV] = 1 \end{cases} \tag{3}$$

where $R$ is the gas constant, $T$ is absolute temperature, $F$ is the Faraday number, and $n = 1$.

Solving this set of equations gives the concentrations of the four states as a function of $E_h$:

$$I = \frac{\exp[a(2E_h - E_m^{Cu_A} - E_m^{Fe_a} - \delta_1 - \delta_2)]}{Y} \tag{4}$$

$$II = \frac{\exp[a(E_h - E_m^{Fe_a} - \delta_1 - \delta_2)]}{Y} \tag{5}$$

$$III = \frac{\exp[a(E_h - E_m^{Cu_A} - \delta_2)]}{Y} \tag{6}$$

$$IV = \frac{1}{Y} \tag{7}$$

where

$$Y = 1 + \exp[a(E_h - E_m^{Fe_a} - \delta_1 - \delta_2)] + \exp[a(E_h - E_m^{Cu_A} - \delta_2)] + \exp[a(2E_h - E_m^{Cu_A} - E_m^{Fe_a} - \delta_1 - \delta_2)] \tag{8}$$

and $a = nF/RT$.

By use of these solutions, the redox potential dependence of the populations of three- and four-electron reduced enzyme can be expressed as

$$3e^- \text{ enzyme} = II + III = \frac{\exp[a(E_h - E_m^{Fe_a} - \delta_1 - \delta_2)] + \exp[a(E_h - E_m^{Cu_A} - \delta_2)]}{Y} \tag{9}$$

$$4e^- \text{ enzyme} = IV = \frac{1}{Y} \tag{10}$$

*"Light Titration" (Backflow) Model.* A flash of light will photolyze the $Fe_{a3}$−CO bond, causing the $E_m$ of $Fe_{a3}$ to drop and freeing electrons to redistribute in the enzyme (*29*, *36*, *37*) as shown in Scheme 2. The left side of the scheme shows the situation in the dark, before the flash. The CO-bound states (I−IV) are the same as those described in Scheme 1

Scheme 2

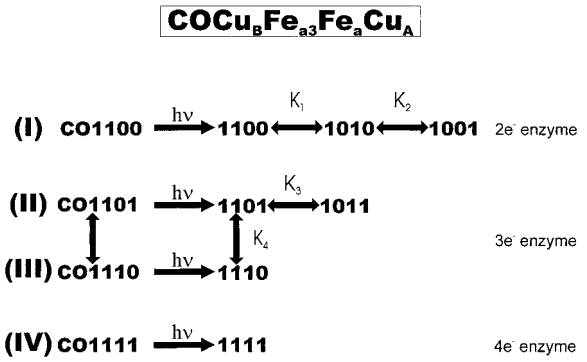


(the same representation is used). The flash converts the CO-bound states to the corresponding unliganded states (second column from left). The partially reduced states (I−III) are now free to evolve by *intramolecular* electron-transfer governed by the following equilibrium constants:

$$K_1 = \exp[a(E_m^{Fe_a} - E_m^{Fe_{a3}})] \quad (11)$$

$$K_2 = \exp[a(E_m^{Cu_A} - E_m^{Fe_a})] \quad (12)$$

$$K_3 = \exp[a[E_m^{Cu_A} - (E_m^{Fe_a} + \delta_1)]] \quad (13)$$

$$K_4 = \exp[a[(E_m^{Fe_a} + \delta_2) - E_m^{Fe_{a3}}]] \quad (14)$$

In the two-electron reduced enzyme, the amount of $Cu_A$ that becomes reduced after the flash is given by

$$Cu_{II} = [I]\frac{K_1K_2}{1 + K_1 + K_1K_2} \quad (15)$$

In the three-electron reduced enzyme, $Cu_A$ is already partially reduced before the flash—it is fully reduced in state II but oxidized in state III. The extent of additional reduction of $Cu_A$ in these two populations of enzyme after the flash is given by

$$Cu_{III} = ([II] + [III])\frac{K_3K_4}{1 + K_3 + K_3K_4} - [II]\frac{K_3}{1 + K_3 + K_3K_4} \quad (16)$$

Thus, the total increase in the amount of reduced $Cu_A$ caused by electron backflow can be evaluated for any redox potential from

$$Cu = Cu_{II} + Cu_{III} \quad (17)$$

## RESULTS

The time-resolved electrometric method allows the measurement of electrical potential ($\Delta\Psi$) across the phospholipid bilayer with microsecond time resolution, making it possible to observe the development of $\Delta\Psi$ within a single turnover of cytochrome *c* oxidase. We have used this methodology to study the reaction of the reduced enzyme with oxygen, using a modification of the "flow-flash" experiment, where, to obtain the requisite time resolution, oxygen is added to the CO-inhibited enzyme in the dark, and the reaction is initiated rapidly by photolyzing the CO (*9*).

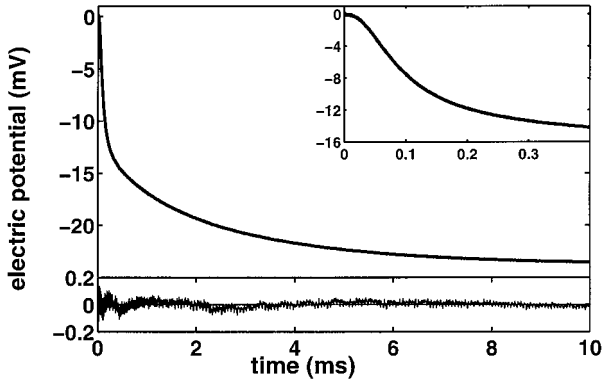


FIGURE 2: Membrane potential development during the reaction of fully reduced cytochrome *c* oxidase with oxygen. Main panel, a typical data recording; bottom panel, difference between experimental and theoretical curves; inset, early part of reaction expanded so that lag can be clearly seen. Conditions: 100 mM HEPES, pH 8, 0.5 $\mu$M cytochrome *c*, 10 $\mu$M hexaammineruthenium, 100 $\mu$M TMPD, 100 $\mu$M DCPIP, 60 mM ferrocyanide, 50 mM glucose, 50 $\mu$g/mL catalase, and 130 $\mu$g/mL glucose oxidase. Reaction started 200 ms after injection of 50 $\mu$L of oxygen-saturated buffer ($[O_2]$ = 1.2 mM). The fit gave the following parameters for the theoretical curve: R → A, $1.03 \times 10^5$ s$^{-1}$ with zero amplitude; A → P − 3.86 $\times 10^4$ s$^{-1}$ and +0.42 mV; P → F, $1.27 \times 10^4$ s$^{-1}$ and −12.62 mV; first F → O, $1.41 \times 10^3$ s$^{-1}$ and −4.51 mV; second F → O, $2.4 \times 10^2$ s$^{-1}$ and −7.03 mV.

An electrometric recording of the reaction of the fully reduced enzyme with oxygen is shown in the main panel of Figure 2. The bottom panel shows the difference between the experimental data and a theoretical fit based on the sequential reaction model described in Materials and Methods. The early part of the reaction is taken up by an initial lag (Figure 2, inset), after which $\Delta\Psi$ develops in three phases. The lag is too long to be caused by a single reaction step. In the fit shown, the lag has been modeled as two sequential steps, the first with a time constant of 6−10 $\mu$s and the second 25−40 $\mu$s. Spectroscopic measurements on the same reaction have found two processes with very similar rate constants, which were assigned as the initial binding of oxygen to $Fe_{a3}$ to form the ferrous-oxy intermediate (A) followed by the transition from A to a formal peroxy intermediate (P). In our fit, the amplitude of the first reaction in the lag was defined as zero. The amplitude of the second reaction was allowed to float, but even so, the fit found it to have a very small, positive, value [3.1% ± 1.5% ($n$ = 14) of the total amplitude],[3] whereas all other phases are negative in sign. This confirms that very little, if any, net charge movement occurs during this part of the reaction.

After the lag $\Delta\Psi$ begins to grow. The fastest component of this increase has a time constant of about 60−100 $\mu$s and contributes 52.6% ± 5.3% of the total amplitude of the response. This corresponds to the third phase of the sequential fit, but since it is the first large increase in $\Delta\Psi$, we will refer to it as the "fast" phase. The rate of this phase is similar to the rate of the process spectroscopically assigned to the transition of P to the ferryl intermediate (F).

This is followed by two "slow" phases with time constants of 0.5−1 ms and 1−5 ms, respectively, which together make up the remaining amplitude (50.5% ± 4.1% of the total; the sum of fast and slow phase amplitudes is slightly larger than

[3] Values are given as percent of total amplitude (start to maximum amplitude) ± standard deviation in the same units.

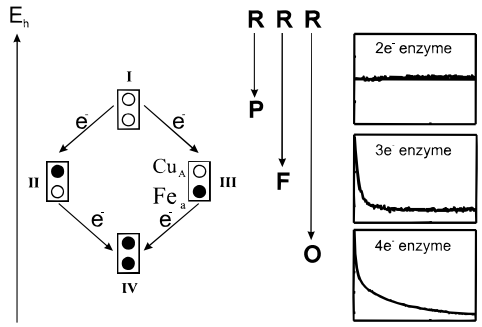


FIGURE 3: Relationship between qualitative electrometric response (right-hand side of the figure) and redox state of the enzyme (left-hand side of the figure). Redox state of the enzyme was manipulated by changing the redox potential of the medium. The experimental curves in the frames were obtained at $E_h = 350$ mV ($2e^-$ enzyme), 320 mV ($3e^-$ enzyme) and 100 mV ($4e^-$ enzyme). Experimental conditions are the same as in Figure 2.

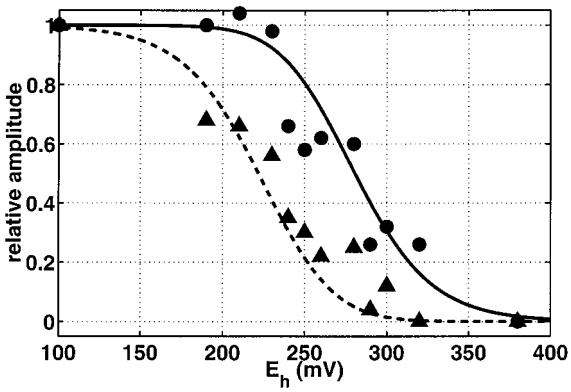


FIGURE 4: Redox titration of fast (●) and slow (▲) phases of the electrometric response. The amplitudes of the phases have been normalized to the corresponding amplitudes in the data at redox potential +100 mV. The solid line shows the theoretical redox dependence of the enzyme population with at least three electrons (sum of eqs 9 and 10); the dashed line shows the four-electron-reduced enzyme population (eq 10), calculated using the "dark titration" model (Materials and Methods) with the following parameters: $E_m{}^{Fe_{a3}} = 330$ mV, $E_m{}^{Fe_a} = 342$ mV, $E_m{}^{Cu_A} = 270$ mV, $\delta_1 = -90$ mV, and $\delta_2 = -20$ mV.

100 percent because of the small positive contribution of the second lag phase). Two phases with approximately the same rates as these are seen in optical studies of the reaction of fully reduced cytochrome *c* oxidase with oxygen. On the basis of their visible spectra, both phases reflect conversion of F to the oxidized form of the enzyme (O) (M. I. Verkhovsky and J. E. Morgan, unpublished results; see also refs *38* and *39*).

When the four-electron reduced enzyme reacts with oxygen, the reaction passes through intermediates P and F to ultimately produce the oxidized enzyme (O). It is possible, however, to control how far along this sequence of intermediates the reaction proceeds by choosing the number of reducing equivalents initially in the enzyme (*40*−*42*). If the enzyme initially contains three electrons, the reaction only goes as far as F, whereas if the enzyme contains two electrons, the reaction is trapped at P (Figure 3).

We used this behavior to help assign the electrometrically observed phases, making measurements with the enzyme at various levels of reduction. In practice, this was done by varying the redox potential ($E_h$) of the medium with which the enzyme is in equilibrium prior to the start of the reaction. In the presence of CO, the two-electron reduced state is stable at relatively high redox potentials. Lowering the potential leads to populations of three- and then four-electron reduced enzyme (left-hand side of Figure 3). Thus, by making measurements beginning with the enzyme poised at different redox potentials, we were able to separate the electrometrically observed phases.

Figure 3 (right-hand side) shows examples of the time course of $\Delta\Psi$ development when cytochrome *c* oxidase, poised at three different initial redox potentials, reacts with oxygen. At high redox potential (about 350 mV vs NHE and higher), CO-bound enzyme contains only two redox electrons, both of which are held in the binuclear center by CO, while the other two centers ($Cu_A$ and $Fe_a$) remain oxidized (state I in Figure 3 and Scheme 1). When this two-electron reduced enzyme reacts with oxygen, the reaction proceeds only as far as the P intermediate. Figure 3 ($2e^-$ enzyme trace) shows that, to a first approximation, no net charge movement takes place in this part of the reaction.

At slightly lower redox potential, some of the enzyme will contain a third electron on either $Cu_A$ or $Fe_a$ (Figure 3, states II and III). Electrometric recordings of the oxygen reaction starting at redox potentials close to 320 mV (Figure 3, $3e^-$ enzyme trace) show the appearance of the "fast" phase (defined above), which was not present in the reaction of the two-electron reduced enzyme, clearly demonstrating that this fast phase is associated with the P to F transition. As the redox potential is lowered further, a population of four-electron reduced enzyme appears. The amplitude of the fast phase increases and the "slow" phase appears, reflecting the fact that in the four-electron reduced population of enzyme, the reduction of oxygen to two waters can proceed to completion, with formation of the fully oxidized enzyme (O). Further lowering of the redox potential increases this four-electron population, further increasing the amplitudes of both fast and slow phases (Figure 3, $4e^-$ enzyme trace).

In this system the two- and four-electron reduced states of the enzyme can be obtained in essentially 100% yield as a starting point for the reaction, but the three-electron reduced enzyme is always an equilibrium mixture of two-, three-, and four-electron reduced species (scheme in Figure 3). Thus, to further confirm the three-electron result, a control experiment was done with cytochrome $bo_3$ oxidase from *Escherichia coli*, which had been prepared in such a way that bound quinol was removed (*43*). Since this preparation contains neither $Cu_A$ nor bound quinol, the fully reduced enzyme contains only three reducing equivalents. When this enzyme reacts with oxygen, the development of $\Delta\Psi$ (data not shown) takes place with essentially the same time course as in the bovine cytochrome *c* oxidase poised at the three-electron level (Figure 3, $3e^-$ enzyme trace), confirming the assignment of the fast electrometric phase to the P to F transition.

A complete titration of the initial redox state of the enzyme is shown in Figure 4. Circles show the amplitude of the fast phase, and triangles show the combined amplitude of the two slow phases. Amplitudes of the phases were normalized to the amplitude of the corresponding phase for the reaction of the fully reduced enzyme (i.e., the lowest redox potential experimentally achieved). The curves show the amplitudes of the fast and slow phases as predicted by a model in which the three-electron reduced enzyme reacts to give only the fast phase while the four-electron reduced enzyme gives both

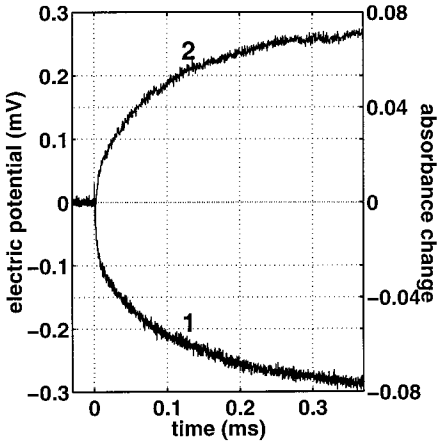


FIGURE 5: Comparison of electron backflow reactions measured by optical spectroscopy at 445 nm (curve 1, right axis) and by the electrometric method (curve 2, left axis). Both curves were measured at the three-electron reduction level of the enzyme ($E_h$ = +270 mV); in both cases corresponding traces for the fully reduced enzyme were subtracted. Optical measurements were carried out on the detergent-solubilized enzyme; conditions 8 $\mu$M cytochrome *c* oxidase, 0.1% dodecyl maltoside, 100 mM BTP, pH 7, 8 $\mu$M cytochrome *c*, 1 mM CO, light path 1 cm (see Materials and Methods). Electrometric conditions were as in Figure 2.

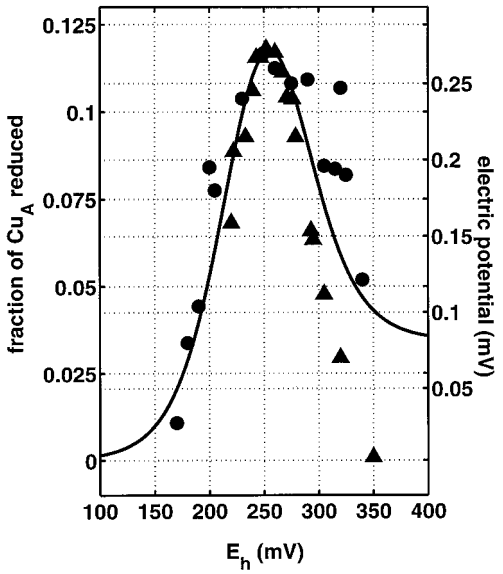


FIGURE 6: Extent of additional reduction of $Cu_A$ after photolysis of CO under anaerobic conditions: optical and electrometric measurements. Reduction of $Cu_A$ as a function of redox potential, determined optically (▲, left axis) aligned with the corresponding electrometric response (●, right axis). Conditions were as in Figure 5; solid line shows predictions of a theoretical calculation based on the "light titration" model (Materials and Methods) using the same parameters as in Figure 4.

fast and slow phases. In this model, the occupancies of various initial redox states in the enzyme sample, as a function of $E_h$, were calculated on the basis of redox potentials and redox interactions as described in the "dark titration" (Materials and Methods).

These electrometric data show that essentially all of the $\Delta\Psi$ generated in the reaction of oxygen with the reduced enzyme is associated with the transitions from P to F and F to O intermediates. However, the data do not give, directly, the number of charges that move across the vesicle membrane in these steps. An independent calibration is needed to define how many millivolts in the electrometric measurement correspond to one charge (*q*) transferred across the membrane. There is another well-characterized electron transfer reaction in the enzyme, which may be able to provide this calibration. When the partially reduced CO-bound enzyme is photolyzed in the absence of oxygen, electrons redistribute in the enzyme (*36*). In an initial fast process ($\tau \sim 3$ $\mu$s) electrons move from $Fe_{a3}$ to $Fe_a$. Then, in a slower process ($\tau \sim 35$ $\mu$s) electrons are further redistributed to $Cu_A$ (*29*, *37*). The extent to which $Cu_A$ becomes reduced varies, depending on the initial redox state of the enzyme, reaching a maximum at the three-electron reduction level. As illustrated in the "electron backflow" panel of Figure 1, only this latter process is expected to involve charge movement in the membrane normal and thus be observable by electrometry.

Figure 5 confirms that the electron backflow process can indeed be observed electrometrically. Trace 1 shows the results of an optically monitored experiment at 445 nm, while trace 2 shows the results of a corresponding electrometric experiment. In both cases, the data for the fully reduced enzyme have been subtracted from data for the partially reduced enzyme ($E_h$ = 270 mV, approximately the point at which the population of the three-electron reduced enzyme is maximum). The optical and electrometric traces follow almost exactly the same time course, indicating similarity of the observed processes. By use of optical data it is possible to calculate the number of electrons transferred to $Cu_A$, and thus, by comparing the optical and electrometric data it should be possible to use the electrometric backflow measurements as a "ruler" to calibrate the amplitudes from the electrometric oxygen reaction data, provided that we know what fraction of the membrane dielectric electrons traverse when $Cu_A$ becomes reduced in the backflow reaction.

The extent of reduction of $Cu_A$ in the backflow reaction depends on the initial redox state of the enzyme. As described above, this amplitude reaches a maximum approximately at the point that the three-electron reduced enzyme population is largest. To use the amplitudes of the optical and electrometric data for calibration, it was necessary to ensure that the enzyme was in the same redox state for both types of measurements. To accomplish this, titrations of both systems were performed in separate, parallel experiments (see Materials and Methods). The results are compared in Figure 6; the triangles represent the fraction of $Cu_A$ that becomes reduced, determined from optical measurements, while the circles represent the amplitudes from separate electrometric measurements. The curve was calculated on the basis of the "light titration" model of the backflow process using the same midpoint potentials and redox interactions used in the "dark titration" model (Materials and Methods). At high $E_h$ values, the electrometric points are much closer to the theoretical curve than the optical points. This is probably because the backflow process includes additional slow heme-to-heme electron redistribution phases (*44*). At 605 nm, this slower phase is opposite in sign to the 35 $\mu$s phase and may thus partially mask this phase in the two-exponential fit, at high $E_h$, when it has a small amplitude.

To use these data to calibrate the electrometric measurements of the oxygen reaction, the same sample that was used for the electrometric backflow measurements was subsequently allowed to reach full reduction and the oxygen

reaction was then carried out. This removes any uncertainty about sample-to-sample variation in the membrane preparation.

The results of the three types of measurements—optical, electrometric backflow and electrometric oxygen reaction—allow us to make the following calculation: At the maximum point, 12% of $Cu_A$ becomes reduced in the backflow reaction. The corresponding electrometric signal was measured as 0.27 mV. Before this can be compared to the electrometric response from the oxygen reaction, it must be normalized to 100% yield. If an electron were transferred to $Cu_A$ in every enzyme molecule, instead of only 12% of the sample, the electrometric signal would be 2.25 mV. The total electrometric amplitude for the oxygen reaction in the same sample was 24 mV or 10.9 times the normalized backflow amplitude. In duplicate samples, ratios of 11.3 and 10.6 were obtained, giving a mean of 10.9 for three trials. Thus, the flow-flash reaction of the fully reduced enzyme with oxygen leads to approximately 10.9 times as much charge being translocated across the membrane as does electron transfer from the hemes of the enzyme to $Cu_A$ in the backflow reaction.

## DISCUSSION

The present work confirms the results of our earlier electrometric study (*22*), which showed that when fully reduced cytochrome oxidase reacts with oxygen, essentially all $\Delta\Psi$ generated in this oxidative portion of the catalytic cycle (R → O) comes from the steps P → F and F → O, and that these two steps make approximately equal contributions to $\Delta\Psi$. The studies on reactions of partially reduced enzyme confirm the correspondence between the fast and slow electrometric phases and the spectroscopically assigned P → F and F → O transitions. The reaction of the three-electron reduced enzyme with oxygen halts at F (*41*, *42*). In electrometric measurements of this reaction, the growth of $\Delta\Psi$ stops after the fast phase; the slow phase is not observed. The reaction of the two-electron reduced enzyme with oxygen halts at P (*40*). This reaction produces no $\Delta\Psi$—neither the fast phase nor the slow phases are observed. This demonstrates that the fast electrometric phase arises from the P → F transition and that the slow phases arise from the F → O transitions and rules out the possibility that these assignments are artifacts of timing. The equality of the P → F and F → O amplitudes also rules out a mechanism proposed by Michel (*45*), according to which a different number of protons is translocated in each these two steps.

Oliveberg et al. (*46*) used pH indicator dyes to study proton uptake during the reaction of the fully reduced, solubilized enzyme with oxygen and found that the consumption of protons takes place with a similar time course to the one found here for the growth of $\Delta\Psi$. Essentially all net proton uptake in this reaction takes place in two phases of approximately equal amplitude, which correspond kinetically to the spectroscopically observed P → F and F → O transitions. This parallel between the time course of proton uptake and that of $\Delta\Psi$ formation suggests close mechanistic linkage between the process of protons translocation and the consumption of protons to make water in the oxygen reaction. This is consistent with the idea that the protons taken up to make water in some sense displace the pumped protons from their sites in the proton translocation machinery (*47*−*49*).

The relative amount of charge translocated during the reaction of fully reduced enzyme with oxygen can also be determined from these electrometric results. For a calibration, we used the well-characterized "backflow" of electrons from $Fe_a$ to $Cu_A$ that takes place upon photolysis of the CO from the enzyme. As described above, measurements on these two types of reaction allow us to establish the relationship between the net amount of charge that moves in the membrane during the oxygen reaction and the amount of charge that moves in the backflow reaction. Approximately 11 times as much charge translocation takes place in the reaction of the fully reduced enzyme with oxygen as in reduction of $Cu_A$ in the backflow reaction (when normalized to 100% yield). In the reaction of the fully reduced enzyme with oxygen, the P → F and F → O steps are each associated with transfer of approximately 0.5 electron from $Cu_A$ to $Fe_a$ (*8*; see introduction). When the contribution of this electron transfer is subtracted, we find that the amount of electrical charge translocated across the membrane in each of these reaction steps amounts to 5 times the charge translocated by electron transfer between $Cu_A$ and $Fe_a$.

Zaslavsky et al. (*39*) used an electrometric measurement system similar to ours, together with quite different chemistry, to study the F → O transition specifically. The F form of the enzyme was prepared by addition of hydrogen peroxide, and tris(bipyridyl)ruthenium [$Ru(bipy)_3$] was used to photoinject an electron into the enzyme. The electron travels via $Cu_A$ to $Fe_a$ and hence to the oxygen-reduction site, where it reduces F to O. Two electrogenic phases were observed, corresponding to fast electron transfer from $Cu_A$ to $Fe_a$ followed by slower reduction of F to O. The amplitude of $\Delta\Psi$ generated in the F → O transition was found to be 4 times the amplitude of the fast phase, which is less than the factor of 5 observed in the present experiments (see above). The photoinjection method has the advantage that the calibration is obtained from the same recording as the measured event, but to be effective this calibration depends on complete formation of intermediate F in the entire enzyme population. If some fraction of the enzyme is not in the F state, electrons from $Ru(bipy)_3$ will still reduce $Fe_a$, but no reduction of F to O will take place. This would lead to an underestimation of the amount of translocated charge. Furthermore, the chemistry by which F is formed with peroxide is still not completely understood, but when peroxide reacts it apparently carries its protons with it into the binuclear site of the enzyme (*50*). It is therefore possible that, even though the F species produced in this way is spectroscopically similar to the true reaction intermediate, the details of protonation within the enzyme are different. This could lead to a lower charge translocation stoichiometry.

To proceed beyond this point, to calculate the actual amount of electrical charge translocation that occurs during the oxygen reaction, it is clearly necessary to know what fraction of the membrane dielectric electrons cross when they move between $Cu_A$ and $Fe_a$, or in other words, how far the different centers are buried in the membrane dielectric. X-ray crystal structure models of the enzyme (*5*, *6*) place $Cu_A$ close to the membrane surface. $Fe_a$ and $Fe_{a3}$ are both buried at a similar depth but appear to be geometrically closer to the outer surface than to the inner surface. Michel (*45*) has estimated the distance from $Fe_a$ to the outer and inner membrane surfaces as approximately 20 and 35 Å, respec-

tively, and further pointed out that the nature of the enzyme structure between $Fe_a$ and the outer side of the membrane appears to be more polar than between $Fe_a$ and the inner side.

Electrical measurements confirm that $Cu_A$ resides outside of the membrane (*51*, *52*). However, in a study on the effect of $\Delta\Psi$ on the apparent midpoint redox potential of $Fe_a$ in CO-inhibited mitochondria, Hinkle and Mitchell (*53*) found that this center behaves as if it were buried approximately halfway through the membrane dielectric. We now define $d_{HM}$, the Hinkle−Mitchell parameter, as the fraction of the total membrane dielectric between the outside medium and $Fe_a$. Originally, $d_{HM}$ was determined to be 0.43 or 0.50 in titrations of the midpoint redox potential of $Fe_a$ with $K^+$ and $H^+$ diffusion potentials, respectively (*53*). Michel (*45*) recently adjusted these values on the basis that the midpoint potential of $Fe_a$ is slightly pH-dependent in CO-inhibited cytochrome *c* oxidase and thus arrived at $d_{HM}$ values of 0.33 and 0.41. However, this correction implicitly assumes that, in the CO-inhibited state, the redox potential of $Fe_a$ depends on the pH of the solution on the negatively charged, *inner*, side of the membrane. This disagrees with the finding by Mitchell (*54*) that, in CO-inhibited mitochondria, the redox potential of $Fe_a$ depends on the pH of the *outside* medium. With this taken into account, the correction would take the opposite sign, increasing rather than decreasing the value of $d_{HM}$.

In conclusion, the present results show unequivocally that, during the reaction of cytochrome *c* oxidase with oxygen, an equal number of charges are translocated across the membrane in the P to F and F to O phases, while the transitions R → A → P make almost no net contribution to the membrane potential. The total number of electrical charges translocated in each of the P → F and F → O transitions is $5.5d_{HM}$. The amount of this translocated charge that can be attributed to electron transfer from $Cu_A$ to $Fe_a$, in each step, is $0.5d_{HM}$, which leaves $5.0d_{HM}$ equivalents of translocated charge due to proton pumping and to electrogenic proton uptake to form water. If we assume that the protons taken up to form water have to cross $1-d_{HM}$ of the dielectric and that one proton is taken up in each reaction step (*52*), then the number of charges translocated due to proton pumping alone is $6d_{HM} - 1$ in each step. The original $d_{HM}$ value of 0.50 (*53*) then leads to the conclusion that all four protons are translocated in the P → F and F → O transitions, in agreement with predictions from equilibrium experiments (*21*). However, if, for example, only one proton is translocated in each of these steps (see refs *46* and *55*), and the two other protons are translocated during the reduction of the enzyme, $d_{HM}$ would have to have a value of 0.33. Clearly, new independent measurements of the value of the Hinkle-Mitchell parameter would be of utmost importance for a reliable assessment of the mechanism of proton translocation by the enzyme.

## ACKNOWLEDGMENT

We thank the following people who helped us to design and construct apparatus for these measurements: Dr. Nikolai Belevich, Matti Lehtinen, Juha Junel, and Martti Heikkinen.

## REFERENCES

1. Puustinen, A., Finel, M., Virkki, M., and Wikström, M. (1991) *Biochemistry 30*, 3936−3942.
2. Wikström, M. (1977) *Nature 266*, 271−273.
3. Hosler, J. P., Ferguson-Miller, S., Calhoun, M. W., Thomas, J. W., Hill, J., Lemieux, L., Ma, J., Georgiou, C., Fetter, J., Shipleigh, J., Tecklenburg, M. M. J., Babcock, G. T., and Gennis, R. B. (1993) *J. Bioenerg. Biomembr. 25*, 121−135.
4. Gennis, R., and Ferguson-Miller, S. (1995) *Science 269*, 1063−1064.
5. Iwata, S., Ostermeier, C., Ludwig, B., and Michel, H. (1995) *Nature 376*, 660−669.
6. Tsukihara, T., Aoyama, H., Yamashita, E., Tomizaki, T., Yamaguchi, H., Shinzawa−Itoh, K., Nakashima, R., Yaono, R., and Yoshikawa, S. (1995) *Science 269*, 1069−1074.
7. Pan, L. P., Hazzard, J. T., Lin, J., Tollin, G., and Chan, S. I. (1991) *J. Am. Chem. Soc. 113*, 5908−5910.
8. Hill, B. C. (1991) *J. Biol. Chem. 266*, 2219−2226.
9. Gibson, Q. H., and Greenwood, C. (1963) *Biochem. J. 86*, 541−555.
10. Oliveberg, M., Brzezinski, P., and Malmström, B. G. (1989) *Biochim. Biophys. Acta, 977*, 322−328.
11. Verkhovsky, M. I., Morgan, J. E., and Wikström, M. (1994) *Biochemistry 33*, 3079−3086.
12. Hill, B. C., and Greenwood, C. (1984) *Biochem. J. 218*, 913−921.
13. Han, S., Ching, Y. C., and Rousseau, D. L. (1990a) *Proc. Natl. Acad. Sci. U.S.A. 87*, 2491−2495.
14. Hill, B. C. (1994) *J. Biol. Chem. 269*, 2419−2425.
15. Morgan, J. E., Verkhovsky, M. I., and Wikström, M. (1994) *J. Bioenerg. Biomembr. 26*, 599−608.
16. Varotsis, C., and Babcock, G. T. (1990) *Biochemistry 29*, 7357−7362.
17. Ogura, T., Takahashi, S., Hirota, S., Shinzawa-Itoh, K., Yoshikawa, S., Appleman, E. H., and Kitagawa, T. (1993) *J. Am. Chem. Soc. 115*, 8527−8536.
18. Han, S., Ching, Y. C., and Rousseau, D. L. (1990b) *Nature 348*, 89−90.
19. Wikström, M. (1981) *Proc. Natl. Acad. Sci. U.S.A. 78*, 4051−4054.
20. Wikström, M., and Morgan, J. E. (1992) *J. Biol. Chem. 267*, 10266−10273.
21. Wikström, M. (1989) *Nature 338*, 776−778.
22. Verkhovsky, M. I., Morgan, J. E., Verkhovskaya, M. L., and Wikström, M. (1997) *Biochim. Biophys. Acta 1318*, 6−10.
23. Hartzell, C. R., and Beinert, H. (1974) *Biochim. Biophys. Acta 368*, 318−338.
24. Baker, G. M., Noguchi, M., and Palmer, G. (1987) *J. Biol. Chem. 262*, 595−604.
25. Finel, M., and Wikström, M. (1986) *Biochim. Biophys. Acta 851*, 99−108.
26. Rigaud, J.-L., Pitard, B., and Levy, D. (1995) *Biochim. Biophys. Acta 1231*, 223−246.
27. Drachev, L. A., Jasaitis, A. A., Kaulen, A. D., Kondrashin, A. A., Liberman, E. A., Nemecek, I. B., Ostroumov, S. A., Semenov, A. Yu., and Skulachev, V. P. (1974) *Nature 249*, 321−324.
28. Drachev, L. A., Kaulen, A. D., Semenov, A. Yu., Severina, I. I., and Skulachev, V. P. (1979) *Anal. Biochem. 96*, 250−262.
29. Verkhovsky, M. I., Morgan, J. E., and Wikström, M. (1992) *Biochemistry 31*, 11860−11863.
30. Dutton, P. L., Wilson, D. F., and Lee, C. P. (1970) *Biochemistry 9*, 5077−5082.
31. Vanneste, W. H. (1966) *Biochemistry 5*, 838−848.
32. Wikström, M., Krab, K., and Saraste, M. (1981) *Cytochrome Oxidase: A Synthesis*, Academic Press, London.
33. Blair, D. F., Ellis, W. R., Jr., Wang, H., Gray, H. B., and Chan, S. I. (1986) *J. Biol. Chem. 261*, 11524−11537.
34. Ellis, W. R. Jr., Wang, H., Blair, D. F., Gray, H. B., and Chan, S. I. (1986) *Biochemistry 25*, 161−167.
35. Wang, H. W., Blair, D. F., Ellis, W. R., Jr., Gray, H. B., and Chan, S. I. (1986) *Biochemistry 25*, 167−171.
36. Boelens, R., Wever, R., and van Gelder, B. F. (1982) *Biochim. Biophys. Acta 682*, 264−272.

37. Oliveberg, M., and Malmström, B. G. (1991) *Biochemistry 30*, 7053−7057.
38. Nilsson, T. (1992) *Proc. Natl. Acad. Sci. U.S.A. 89*, 6497−6501.
39. Zaslavsky, D., Kaulen, A. D., Smirnova, I. A., Vygodina, T., and Konstantinov, A. A. (1993) *FEBS Lett. 336*, 389−393.
40. Chance, B., Saronio, C., and Leigh, J. S. (1975) *J. Biol. Chem. 250*, 9226−9237.
41. Witt, S. N., and Chan, S. I. (1987) *J. Biol. Chem. 262*, 1446−1448.
42. Lauraeus, M., Morgan, J., and Wikström, M. (1993) *Biochemistry 32*, 2664−2670.
43. Puustinen, A., Verkhovsky, M. I., Morgan, J. E., Belevich, N. P., and Wikström, M (1996) *Proc. Natl. Acad. Sci. U.S.A. 93*, 1545−1548.
44. Hallén, S., Brzezinski, P., and Malmström, B. (1994) *Biochemistry 33*, 1467−1472.
45. Michel, H. (1998) *Proc. Natl. Acad. Sci. U.S.A. 95*, 12819−12824.
46. Oliveberg, M., Hallen, S., and Nillson, T. (1991) *Biochemistry 30*, 436−440.
47. Wikstrom, M., Bogachev, A., Finel, M., Morgan, J. E., Puustinen, A., Raitio, M., Verkhovskaya, M., and Verkhovsky, M. I. (1994) *Biochim. Biophys. Acta 1187*, 106−111.
48. Morgan, J. E., Verkhovsky, M. I., and Wikström, M. (1996) *Biochemistry 35*, 12235−12240.
49. Rich, P. R. (1995) *Aust. J. Plant. Physiol. 22*, 479−486.
50. Konstantinov, A. A., Capitanio, N., Vygodina, T. V., and Papa, S. (1992) *FEBS Lett. 312*, 71−74.
51. Rich, P. R., West, I. C., and Mitchell, P. (1988) *FEBS Lett. 233*, 25−30.
52. Mitchell, R., Mitchell, P., and Rich, P. R. (1992) *Biochim. Biophys. Acta 1101*, 188−191.
53. Hinkle, P., and Mitchell, P. (1970) *Bioenergetics 1*, 45−60.
54. Mitchell, R. (1991) Ph.D. Thesis, University of London, England.
55. Nilsson, T., Hallen, S., and Oliveberg, M. (1990) *FEBS Lett. 260*, 45−47.

BI982275L